THE ASTROPHYSICAL JOURNAL, 536:L85–L88, 2000 June 20
© 2000. The American Astronomical Society. All rights reserved. Printed in U.S.A.

NEUTRON-CAPTURE ELEMENT ABUNDANCES IN THE GLOBULAR CLUSTER M15[1]

CHRISTOPHER SNEDEN,[2] JENNIFER JOHNSON,[3,4] ROBERT P. KRAFT,[3] GRAEME H. SMITH,[3]
JOHN J. COWAN,[5] AND MICHAEL S. BOLTE[3]
Received 2000 April 18; accepted 2000 May 12; published 2000 June 13

ABSTRACT

High-resolution, high signal-to-noise ratio, blue–violet spectra of three red giant branch tip stars in M15 have been obtained with the Keck I High-Resolution Echelle Spectrograph. These spectra have been analyzed to determine the abundances of several neutron-capture elements, including the radioactive chronometer element thorium. There are two principal results of this study. First, the abundances of the heavier ($Z \geq 56$) elements for each of the three stars is well matched by a scaled solar system *r*-process abundance distribution. Second, a weighted mean–observed Th/Eu ratio for the stars implies an age for the neutron-capture material in M15 stars of 14 ± 3 Gyr, in reasonable agreement with other recent age estimates for Galactic globular clusters.

Subject headings: globular clusters: individual (M15) — nuclear reactions, nucleosynthesis, abundances — stars: abundances — stars: late-type — stars: Population II

1. INTRODUCTION

The ages of Galactic globular clusters provide the most direct estimates of the age of our Galaxy. Cluster ages have generally been based on detailed comparisons of their color-magnitude diagrams with theoretical isochrones, and they currently range from ≃11 to 16 Gyr (e.g., Chaboyer, Demarque, & Sarajedini 1996; Gratton et al. 1997; Pont et al. 1998; review by VandenBerg, Stetson, & Bolte 1996). A more precise measurement depends on the resolution of several observational/theoretical uncertainties. Cluster white dwarf luminosity functions may provide independent age estimates, but such studies (e.g., Richer et al. 1997) are still in their infancy.

The age of the solar system is determined from analyses of radioactive chronometer elements, and the abundance of thorium ($\tau_{1/2} = 14.0$ Gyr) has been used to estimate stellar ages (e.g., Butcher 1987; François, Spite, & Spite 1993). Recently, Sneden et al. (1996, 2000), Cowan et al. (1999), and Westin et al. (2000) have compared the abundances of Th with a large number of stable *n*-capture elements (*n*-capture: $Z > 30$) to estimate ages of ≃15 Gyr for two very metal-poor but *n*-capture–rich halo field giants. The metal-poor ([Fe/H] ≃ −2.4)[6] globular cluster M15 should be well-suited for similar age studies because a detailed analysis of red-region high-resolution spectra (Sneden et al. 1997) has shown that barium and europium are overabundant in a large fraction of M15 giants. Among these M15 giants, the [Ba/Eu] ratio is substantially less than zero, indicating that *r*(apid)-process *n*-capture synthesis from prior supernovae in the early cluster environment has produced these elements. However, only one Eu II line and three Ba II lines are routinely detectable in the red spectral region of metal-poor giants; the vast majority of strong *n*-capture element transitions occur at shorter wavelengths. To study the *n*-capture element abundances of M15 stars in detail and to attempt to detect Th, we have gathered high-resolution blue–violet spectra of three of the most luminous giants in this cluster. The results of the abundance analyses of these spectra are reported in this Letter.

2. OBSERVATIONS AND ABUNDANCE ANALYSIS

The Keck I High-Resolution Echelle Spectrograph (Vogt et al. 1994) was employed on 1997 September 3 and 4 to obtain spectra of luminous M15 red giants K341, K386, K462, and K583. These stars were selected from the Sneden et al. (1997) study with the criteria that they have closely matched model atmospheric parameters but a large spread in [Ba/Fe] and [Eu/Fe]. The wavelength domain of the spectra gathered for these stars was 3650 Å < λ < 5200 Å. A slit of width 0.″86 was used to give a resolving power of $R \equiv \lambda/\Delta\lambda \simeq 45{,}000$, and the signal-to-noise ratio (S/N) obtained varied from ∼30 at the low-wavelength end of the data to ∼150 at the long-wavelength end. Spectra of a tungsten filament lamp and a Th-Ar hollow cathode lamp, as well as "bias" and "dark" exposures, accompanied the stellar observations. The spectra were reduced with standard echelle reduction procedures using IRAF.[7] Inspection of the final extracted spectrum of K386 revealed that its absorption lines were slightly asymmetrical, characteristic possibly of a binary star (or a chance line-of-sight combination of the light of two M15 stars). This made reliable equivalent width measures doubtful for this star, so it was discarded from further consideration here.

We estimated atmospheric parameters of the program stars via abundance analyses of a set of Fe-peak lines appearing in the 3900 Å < λ < 5200 Å spectral region (shortward of 3900 Å, the line crowding is too great and the spectral S/N is too low for useful analysis). The model parameters were adjusted to satisfy the usual requirements that the derived abundances show no trends with excitation potential (to set $T_{\rm eff}$), ionization

[1] Based on observations obtained with the Keck I Telescope of the W. M. Keck Observatory, which is operated by the California Association for Research in Astronomy (CARA), Inc., on behalf of the University of California, the California Institute of Technology, and NASA.

[2] Department of Astronomy and McDonald Observatory, University of Texas at Austin, RLM 15.308, Austin, TX 78712; chris@verdi.as.utexas.edu, chris@astro.as.utexas.edu.

[3] University of California Observatories, Lick Observatory, Santa Cruz, CA 95064; graeme@ucolick.org, kraft@ucolick.org, bolte@ucolick.org.

[4] Observatories of the Carnegie Institution of Washington, 813 Santa Barbara Street, Pasadena, CA 91101-1292; jennifer@ociw.edu.

[5] Department of Physics and Astronomy, Room 131 Nielsen Hall, University of Oklahoma, Norman, OK 73019-0225; cowan@mail.nhn.ou.edu.

[6] [A/B] ≡ $\log (N_A/N_B)_{\rm star} - \log (N_A/N_B)_\odot$, and $\log \epsilon(A) \equiv \log (N_A/N_H) + 12.0$, for elements A and B.

[7] IRAF is distributed by the National Optical Astronomy Observatories, which are operated by the Association of Universities for Research in Astronomy, Inc., under cooperative agreement with the National Science Foundation.

TABLE 1
M15 Abundances

	log ϵ					[M/H]				
Species	Sun	Sun, *r*	K341	K462	K583	K341	K462	K583	⟨σ⟩[a]	⟨*N*⟩[b]
Ti I	4.99	...	+2.81	+2.85	+2.85	−2.18	−2.14	−2.14	0.10	25
Ti II	4.99	...	+3.00	+3.02	+2.88	−1.99	−1.97	−2.11	0.17	10
V I	4.00	...	+1.48	+1.52	+1.50	−2.52	−2.48	−2.50	0.09	8
Cr I	5.67	...	+3.02	+3.11	+3.02	−2.65	−2.56	−2.65	0.08	8
Fe I	7.52	...	+5.20	+5.27	+5.18	−2.32	−2.25	−2.34	0.09	21
Fe II	7.52	...	+5.30	+5.30	+5.21	−2.22	−2.22	−2.31	0.15	5
Ni I	6.25	...	+3.72	+3.75	+3.74	−2.53	−2.50	−2.51	0.09	9
Zn I	4.60	...	+2.31	+2.30	+2.24	−2.29	−2.30	−2.36	...	1
Y II	2.24	1.66	−0.33	−0.09	−0.53	−2.57	−2.33	−2.77	0.13	4
Zr II	2.60	1.86	+0.73	+0.89	+0.60	−1.87	−1.71	−2.00	0.07	3
Ba II	2.13	1.46	−0.07	+0.06	−0.44	−2.20	−2.07	−2.57	0.19	6
La II	1.22	0.60	−0.67	−0.41	−1.13	−1.89	−1.63	−2.35	0.08	4
Ce II	1.55	0.86	−0.61	−0.41	−0.96	−2.16	−1.96	−2.51	0.13	5
Nd II	1.50	1.18	−0.27	−0.04	−0.68	−1.77	−1.54	−2.18	0.20	7
Sm II	1.00	0.79	−0.80	−0.52	−1.13	−1.80	−1.52	−2.13	0.12	12
Eu II	0.51	0.51	−0.88	−0.61	−1.22	−1.39	−1.12	−1.73	0.09	3
Gd II	0.99	0.99	−0.51	−0.20	−1.03	−1.63	−1.32	−2.15	0.18	2
Dy II	1.10	1.10	−0.25	+0.12	−0.62	−1.35	−0.98	−1.72	0.20	2
Th II	0.12	0.12	−1.47	−1.26	−1.7:	−1.59	−1.38	−1.8:	0.10	2

Note.—For K341, $T_{\rm eff}$ = 4200 K, log g = 0.15, v_t = 2.15, and [M/H] = −2.2. For K462, $T_{\rm eff}$ = 4225 K, log g = 0.15, v_t = 2.10, and [M/H] = −2.2. For K583, $T_{\rm eff}$ = 4275 K,log g = 0.15, v_t = 2.20, and [M/H] = −2.2.

[a] Values of the sample standard deviations, averaged over all three stars.

[b] The average number of transitions employed for all three stars.

stage (for log g), and equivalent width (for v_t). Detailed descriptions of model atmosphere choices, line analysis codes, etc., are given by Sneden et al. (1997). The derived model parameters and Fe-peak element abundances are given in Table 1. For each abundance in each program star, we computed the sample standard deviation σ from the results for multiple absorption lines of a given element. The σ-values for an individual species varied little from star to star, probably indicating that these internal scatter measures are most influenced by feature blending, continuum placement, and transition probability uncertainties. In Table 1, we simply list the mean values per species of $\langle\sigma\rangle$ for the three stars.

The newly derived model parameters are similar to those determined by Sneden et al. (1997) from data that covered the 5500–6700 Å spectral region. The new log g estimates are ∼0.2 lower, the [Fe/H] values are ∼0.1 higher, and the [X/Fe] ratios of the Fe-peak elements are ∼0.2 lower than those determined by Sneden et al. The difference in Fe abundances derived from blue- and red-region lines reemphasizes the difficulty in establishing reliable absolute metallicity scales for globular clusters. Resolution of these discrepancies awaits future analyses of all M15 high-resolution data.

Questions of model atmospheric parameter uncertainties cannot obscure the fact that these three M15 giants are very similar. In Figure 1, we overplot the spectra of these stars in several small wavelength intervals, in order to illustrate the strengths of some features used in the abundance analysis. In this figure (see especially Fig. 1*a*) and everywhere else in the 3900–5200 Å region, the Fe-peak element transitions are virtually indistinguishable from one star to another. This is reflected in the nearly identical derived model atmosphere parameters.

To study the *n*-capture elements, we began with the transitions appearing in the list used in the analysis by Sneden et al. (1996) of the *n*-capture–rich star CS 22892−052. Some of the lines included in the CS 22892−052 analysis are too blended in the M15 spectra and had to be eliminated. But some *n*-capture lines occurring in 4600–5000 Å (not covered in the CS 22892−052 spectra) were added. The *n*-capture abundances were derived from equivalent width or synthetic spectrum analyses (see Sneden et al. 1996 for *gf*-value references and a discussion of analysis techniques).

The *n*-capture abundances are given in Table 1. The σ-values for Ba, Nd, and Dy are significantly larger ($\langle\sigma\rangle \simeq 0.2$) than they are for the other elements. For Nd, we suspect uncertainties in the *gf*-values (see the discussion in Sneden et al. 1996). For Dy, only two lines were used in the analysis, and they were difficult to synthesize (both are blended, and λ4103 lies in the wing of Hδ). Derivation of reliable Ba abundances in M15 giants is not easy, for the Ba II resonance lines (λλ4554, 4934) are very strong (EW > 200 mÅ) and thus very sensitive to the choice of microturbulent velocity. Our analysis, taking full account of the hyperfine and isotopic substructures of all Ba lines, yielded abundances ∼0.3 dex larger than those derived by Sneden et al. (1997) from the red-region lines at 5853, 6141, and 6496 Å. The abundances of two very weak high-excitation lines (at 3891 and 4130 Å) were in reasonable agreement with those of the blue-region resonance lines, but the mean Ba abundances are not very secure.

While bearing in mind the cautions about some *n*-capture abundances, there are very clear differences between the overall *n*-capture abundance levels of the three stars. This is easily seen in the strengths of the transitions of these elements shown in Figure 1 and in the derived abundances given in Table 1. The relative [⟨*n*-capture⟩/Fe] ratios (largest in K462, about 0.3–0.4 dex less in K341, and about the same amount less in K583) are roughly consistent with the [Ba/Fe] and [Eu/Fe] abundances of Sneden et al. (1997) for these three stars. All *n*-capture abundances appear to vary in unison.

In Figure 1*d*, we show the observed line Th II λ4019.1 in the M15 giants. This feature is heavily blended with atomic and molecular (^{13}CH) lines. A clear detection of λ4019.1 is seen in all three giants, but in K583 the contrast between the Th II line and the surrounding contaminants is small enough

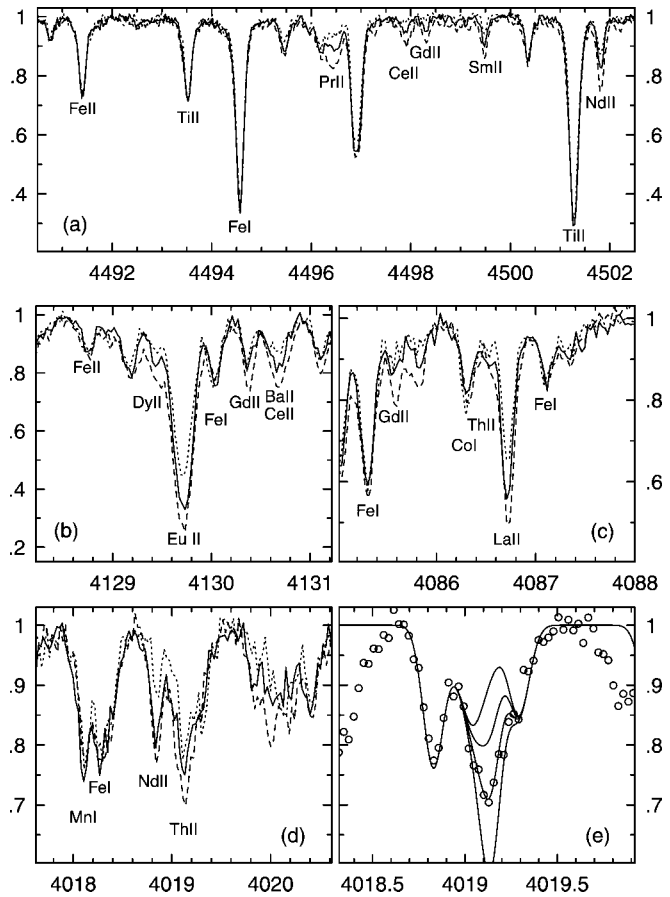

FIG. 1.—(*a–d*): Spectra of three M15 giants in four representative wavelength intervals that were used in the abundance analyses. In these four panels, the dashed line is the spectrum of K462, the solid line that of K341, and the dotted line that of K583. The species responsible for some of the cleaner spectral features are identified. In (*a*), a wavelength region with several prominent Fe-peak neutral and ionized species transitions is displayed; the similarity of the Fe-peak features (e.g., Ti II λ4493.5) indicates essentially identical abundances of these elements in all three stars. In contrast, the strengths of the *n*-capture features [Eu II λ4129.7 in (*b*), La II λ4086.7 in (*c*), and Th II λ4019.1 in (*d*)] have large differences, which are always in the same sense of a progression of increasing strength from K583 to K341 to K462. In (*e*), observed and synthetic spectra of the Th II feature in K462 are shown. The observed spectrum is depicted as open circles, and the four synthetic spectra shown as solid lines are for abundance ratios of [Th/Fe] = $-\infty$, +0.36, +0.86, and +1.36.

to make our Th measurement unreliable. The Th abundances of K341 and K462 are far more trustworthy. In Figure 1*e*, we show synthetic and observed Th spectra of K462, the star with the largest [*n*-capture/Fe] ratio. The Th II line dominates the blend, but the contaminants are not insignificant. The total blended feature was matched iteratively by varying the abundances of the several blending species. Note especially that we set the strengths of the ^{13}CH part of this feature (Norris, Ryan, & Beers 1997) by first employing spectrum syntheses of longer wavelength CH G-band lines in order to determine carbon isotope ratios for these stars (the analysis method and CH features considered are described in Gratton et al. 2000). We derived $\langle ^{12}C/^{13}C\rangle = 5 \pm 2$ for all stars, in good agreement with the very low values found in red giant branch tip giants of other clusters (e.g., Brown & Wallerstein 1989; Suntzeff & Smith 1991; Ivans et al. 1999). Then that isotopic ratio was adopted, and the syntheses of several ^{12}CH lines near 4019 Å were used to determine the strengths of the blending ^{13}CH features near

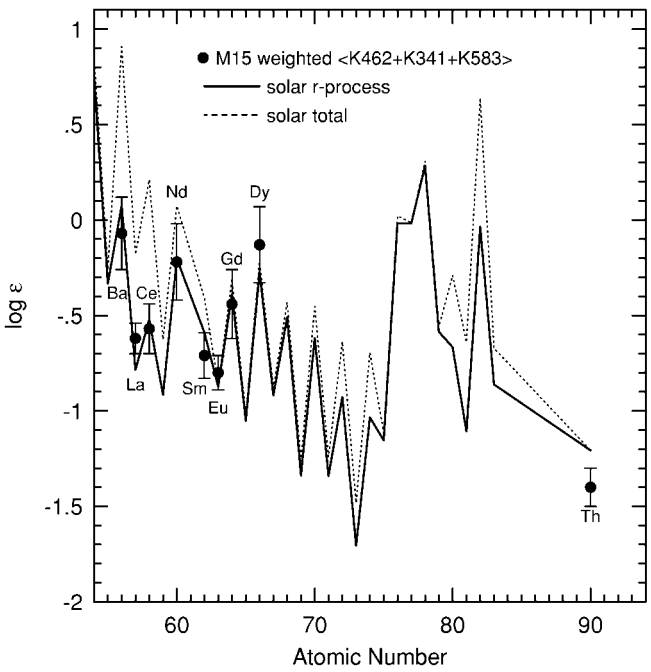

FIG. 2.—Weighted mean abundances of *n*-capture elements with $Z \geq 56$ in M15 giants. In forming the means, the abundances of K462 are given triple weight, K341 double weight, and K583 single weight, to account for the relative [*n*-capture/Fe] abundance levels of these three stars. The solar system *r*-process–only abundance distribution (Burris et al. 2000) has been shifted by its mean difference compared with the M15 points shown in this figure for elements Ba through Dy and has been plotted as a solid curve. The solar system total abundance distribution has been shifted by this same amount and plotted as a dotted line.

the Th II line. A second Th II line at 4086.5 Å is also detectable in M15 giants (Fig. 1*c*), but it is too weak and blended to yield reliable Th abundances.

3. DISCUSSION AND CONCLUSIONS

Our study shows that the abundances of those *n*-capture elements with $Z \geq 56$ in M15 giants are consistent with a pure *r*-process synthesis pattern. We illustrate this in Figure 2, where we plot weighted mean abundances for individual elements. The weighting factors, reflecting the relative [*n*-capture/Fe] ratios of the stars, were chosen to be 3, 2, and 1 for K462, K341, and K583, respectively. These mean log ϵ values are compared in the figure with the solar system *r*-process–only abundances (Burris et al. 2000). The solar system elemental abundances have been shifted by the mean difference (-1.38 ± 0.04; $\sigma = 0.12$) between M15 and solar system abundance distributions for the elements from Ba through Dy.[8] Clearly these abundances match, within observational errors, the solar system *r*-process abundances. The total solar system $r + s$ abundance distribution does not fit the M15 data, and a pure solar system *s*-process abundance set (not depicted in Fig. 2) will deviate even more. We stress that each star individually exhibits the same scaled solar *r*-process abundance pattern. This result adds to the body of evidence already in the literature indicating that heavier *n*-capture elements in the lowest metallicity stars have

[8] The elements Y, Zr, Ba, and Th have been excluded from the averages. The abundances of the lighter elements Y and Zr do not always track the abundances of the heavier *n*-capture elements (e.g., Burris et al. 2000) and indeed may be synthesized in a somewhat different nucleosynthetic process (e.g., Wasserburg, Busso, & Gallino 1996; Cowan et al. 1999).

only weak *s*-process contributions (e.g., McWilliam 1997; Burris et al. 2000).

From the Th abundances of M15 giants we may estimate the "age" of *n*-capture material in this cluster. The weighted mean $\log \epsilon(\mathrm{Th/Eu}) = -0.60$ or $N_{\mathrm{Th}}/N_{\mathrm{Eu}} = 0.25$. This measurement can be compared with theoretical estimates of the initial value of $N_{\mathrm{Th}}/N_{\mathrm{Eu}}$ at the time of the formation of these elements in an *r*-process synthesis event. Cowan et al. (1999) suggested that the most reliable values of this ratio range from 0.48 to 0.55, based on reproducing the observed solar system *r*-process isotopic abundances. Comparing these predicted ratios with the weighted mean M15 value given above leads to age estimates ranging from 13.2 to 15.8 Gyr, with an average value of 14.3 Gyr. The age estimates resulting from the theoretical predictions have an uncertainty on the order of 3 Gyr (Cowan et al. 1999). An additional age determination can be performed by comparing the observed Th/Eu stellar ratios with that of the solar system at time of formation, Th/Eu = 0.463. Such a comparison, which is independent of any theoretical calculations or modeling, gives an age of 12.3 Gyr for the average of the three stars in M15. This age determination, however, is more properly a lower limit since the solar Th/Eu ratio, from a 4.5 Gyr old star, is only a lower limit to the zero-age *r*-process abundances—Eu is stable, but Th has partially decayed. We caution, though, that all of these age estimates have an observational uncertainty on the order of 3 Gyr (equivalent to $\simeq 0.08$ in $\log \epsilon$) that is due to the uncertainties in our abundance determination of the *n*-capture elements (including Th) in these very cool, line-rich M15 giant star blue–violet spectra.

These age estimates effectively bracket other globular cluster age determinations (see the references quoted in § 1) and are consistent with, or slightly less than, Th-based age determinations of metal-poor field halo stars (Westin et al. 2000 and references therein). This "new" cluster age technique probably will be most useful for those clusters that are of lowest metallicity, that have large [*n*-capture/Fe] abundance ratios, and that have *r*-process abundance distributions for the heavier *n*-capture elements. So far, M15 is the only globular cluster known in which such abundance characteristics have been identified. M92, for example, is very metal-poor but has much lower [*n*-capture/Fe] ratios (Armosky et al. 1994). Systematic high-resolution studies of *n*-capture elements in other clusters should be undertaken to find more that are suitable for Th-age analysis.

We thank Inese Ivans and Jim Truran for helpful discussions on this work. We are pleased to acknowledge the support of NSF grants AST 96-18351 to R. P. K. and G. H. S., AST 96-18332 to J. J. C., and AST 96-18364 to C. S.

REFERENCES

Armosky, B. J., Sneden, C., Langer, G. E., & Kraft, R. P. 1994, AJ, 108, 1364
Brown, J. A., & Wallerstein, G. 1989, AJ, 98, 1643
Burris, D. L., Pilachowski, C. A., Armandroff, T. A., Sneden, C., Cowan, J. J., & Roe, H. 2000, ApJ, submitted
Butcher, H. R. 1987, Nature, 328, 127
Chaboyer, B., Demarque, P., & Sarajedini, A. 1996, ApJ, 459, 558
Cowan, J. J., Pfeiffer, B., Kratz, K.-L., Thielemann, F.-K., Sneden, C., Burles, S., Tytler, D., & Beers, T. C. 1999, ApJ, 521, 194
François, P., Spite, M., & Spite, F. 1993, A&A, 274, 821
Gratton, R. G., Fusi Pecci, F., Carretta, E., Clementini, G., Corsi, C. E., & Lattanzi, M. 1997, ApJ, 491, 749
Gratton, R. G., Sneden, C., Carretta, E., & Bragaglia, A. 2000, A&A, 354, 169
Ivans, I. I., Sneden, C., Kraft, R. P., Suntzeff, N. B., Smith, V. V., Langer, G. E., & Fulbright, J. P. 1999, AJ, 118, 1273
McWilliam, A. 1997, ARA&A, 35, 503
Norris, J. E., Ryan, S. G., & Beers, T. C. 1997, ApJ, 489, L169
Pont, F., Mayor, M., Turon, C., & VandenBerg, D. A. 1998, A&A, 329, 87
Richer, H. B., et al. 1997, ApJ, 484, 741
Sneden, C., Cowan, J. J., Ivans, I. I., Fuller, G., Burles, S., Beers, T. C., & Lawler, J. E. 2000, ApJ, 533, L139
Sneden, C., Kraft, R. P., Shetrone, M. D., Smith, G. H., Langer, G. E., & Prosser, C. F. 1997, AJ, 114, 1964
Sneden, C., McWilliam, A., Preston, G. W., Cowan, J. J., Burris, D. L., & Armosky, B. J. 1996, ApJ, 467, 819
Suntzeff, N. B., & Smith, V. V. 1991, ApJ, 381, 160
VandenBerg, D. A., Stetson, P. B., & Bolte, M. 1996, ARA&A, 34, 461
Vogt, S. S., et al. 1994, Proc. SPIE, 2198, 362
Wasserburg, G. J., Busso, M., & Gallino, R. 1996, ApJ, 466, L109
Westin, J., Sneden, C., Gustafsson, B., & Cowan, J. J. 2000, ApJ, 530, 783